Suplemento de la Revista Mexicana de Física **4** 011008 (2023) 1–9

Tri-Bi-Maximal flavor pattern deviation using equivalent class

M. R. Aparicio-Méndez, O. Félix-Beltrán, and F. González-Canales

Facultad de Ciencias de la Electrónica, Benemérita Universidad Autónoma de Puebla, Apartado Postal 542, Puebla, Pue. 72000, México.

E. Barradas-Guevara

Facultad de Ciencias Físico Matemáticas, Benemérita Universidad Autónoma de Puebla, Apartado Postal 1152, Puebla, Pue. 72000, México.

Received 16 November 2022; accepted 10 July 2023

We assume that the neutrino mass matrix $\mathbf{M}_\nu$, in the model-independent context, is diagonalized by the Tri-Bi-Maximal (TBM) pattern. In the following, we explore the TBM mixing pattern deviation by considering different textures for the charged lepton matrix, which are classified into equivalence classes that allow us to reproduce the experimental data on neutrino oscillation. Our target is on the charged lepton matrix with the minimum number of free parameters, *i.e.*, the maximum number of zeros of the texture that allows us to correctly reproduce the value of the reactor mixing angle θ_{13}. We show a deviation from the TBM pattern in terms of the charged leptonic masses, which provides a prediction value for the phase factors in the charged lepton mass matrices. These are related to the "Dirac-like" CP and "Majorana-like" phase factors. For the last type of phase, we show its phenomenological implications through effective Majorana mass in the neutrinoless double-beta decay.

Keywords: Neutrinos; Tri-Bi-Maxima pattern; equivalent classes.

DOI: https://doi.org/10.31349/SuplRevMexFis.4.011008

1. Introduction

The discovery of masses and flavor mixing of the neutrino can be regarded as one of the biggest breakthroughs in the understanding of particle physics. However, this fact provides the first evidence of a beyond the Standard Model physics (BSM) [1]. The experimental discovery of a nonzero reactor mixing angle [2] marked the beginning of a new era in particle physics [3–5]. These experimental results have expanded the flavor structure in the lepton sector by providing us the first indication for a new CP violation source [6]. Relevant works on lepton sector analysis are Refs. [7–12], as Ref. [13].

Nevertheless, neutrino oscillation experiments do not resolve the question of whether neutrinos are Majorana o Dirac particles, or give some information about the absolute neutrino mass scale, or about Majorana phase factors, neither. Majorana phases enter in decay amplitudes that violate the leptonic number, such as neutrinoless double beta decay [14]. Hence, an experimental observation of neutrinoless double-beta decay can test the absolute scale of neutrinos masses and the nature of the neutrino mass term, that is, the neutrinos would be Majorana particles. Now, it is well known that neutrinos have a small value for their masses, less than eV, which naturally can be explained by considering neutrinos as Majorana particles [15].

The TBM pattern [16] considers a maximal atmospheric mixing angle $\theta = 45^o$ and solar angle $\theta_{12} = 35.26^o$, while the reactor angle is postulated as zero. Also, in the TBM framework, the charged lepton mass matrix is considered a diagonal matrix. The TBM flavor pattern was ruled out by the experimental measurement of the reactor angle, which reports a reactor mixing angle of the order of eight degrees [3, 5, 17]. However, all is not lost with respect to the TBM pattern, if we remember that the leptonic mixing matrix $\mathbf{U}_{PMNS}$, arises from the mismatch between diagonalization of the mass matrices of charged leptons and the left-handed neutrinos. Realistic TBM-like neutrino mixing matrix can be reviewed in Refs. [18, 19].

A generalization can be proposed in which the unitary matrix that diagonalizes the neutrino mass matrix is represented by the TBM flavor pattern, while the unitary matrix that diagonalizes the charged lepton mass matrix corresponds to corrections to the reactor, solar and atmospheric mixing angles.

If neutrinos are considered as Majorana particles, the low energy neutrino oscillation phenomenon in the base of flavor eigenstates is given by the Lagrangian

$$\mathcal{L} = -\frac{g}{\sqrt{2}}\overline{\ell}_L\gamma^\mu\nu_L W_\mu - \frac{1}{2}\overline{\nu_R^c}\,\mathbf{M}_\nu\nu_L - \overline{\ell}_R\mathbf{M}_\ell\ell_L + \text{H. c.}. \quad (1)$$

The $\mathbf{M}_\nu$ is the neutrino mass matrix. The $\mathbf{M}_\ell$ is the charged lepton mass matrix. These mass matrices can be rotated to the mass eigenstates basis by means of the unitary transformations.

The mass matrices can be rotated to the mass eigenstates basis by means of the unitary transformations

$$\mathbf{M}_\nu = \mathbf{U}_\nu^*\mathbf{\Delta}_\nu\mathbf{U}_\nu^\dagger \quad \text{and} \quad \mathbf{M}_\ell = \mathbf{V}_\ell\mathbf{\Delta}_\ell\mathbf{U}_\ell^\dagger. \quad (2)$$

Here,

$$\mathbf{\Delta}_\nu = \mathrm{diag}\left(m_{\nu 1}, m_{\nu 2}, m_{\nu 3}\right),$$
$$\mathbf{\Delta}_\ell = \mathrm{diag}\left(m_e, m_\mu, m_\tau\right).$$

The charged currents term takes the form

$$\mathcal{L}_{cc} = -\frac{g}{\sqrt{2}}\overline{\ell}_L \gamma^\mu \nu_L W_\mu,$$
$$\mathcal{L}'_{cc} = -\frac{g}{\sqrt{2}}\overline{\ell'}_L \gamma^\mu \mathbf{U}_{\mathrm{PMNS}} \nu'_L W_\mu, \tag{3}$$

with ${\ell'}_L = \mathbf{U}_\ell \ell_L$ and ${\nu'}_L = \mathbf{U}_\nu \nu_L$. The $\mathbf{U}_{\mathrm{PMNS}}$ matrix is the leptonic flavor mixing matrix and governs the neutrinos and charged lepton couplings

$$\mathbf{U}_{\mathrm{PMNS}} = \mathbf{U}_\ell^\dagger \mathbf{U}_\nu = \begin{pmatrix} U_{e1} & U_{e2} & U_{e3} \\ U_{\mu 1} & U_{\mu 2} & U_{\mu 3} \\ U_{\tau 1} & U_{\tau 2} & U_{\tau 3} \end{pmatrix}. \tag{4}$$

In the symmetric parametrization, $\mathbf{U}_{\mathrm{PMNS}}$ can be write down as

$$\begin{pmatrix} c_{12}c_{13} & s_{12}c_{13}e^{-i\phi_{12}} & s_{13}e^{-i\phi_{13}} \\ -s_{12}c_{23}e^{i\phi_{12}} - c_{12}s_{13}s_{23}e^{-i(\phi_{23}-\phi_{13})} & c_{23}c_{12} - s_{23}s_{12}s_{13}e^{-i(\phi_{12}+\phi_{23}-\phi_{13})} & c_{13}s_{23}e^{-i\phi_{23}} \\ s_{12}s_{23}e^{i(\phi_{12}+\phi_{23})} - c_{12}s_{13}c_{23}e^{i\phi_{13}} & -c_{12}s_{23}e^{i\phi_{23}} - s_{12}s_{13}c_{23}e^{-i(\phi_{12}-\phi_{13})} & c_{13}c_{23} \end{pmatrix}, \tag{5}$$

where $c_{ij} \equiv \cos\theta_{ij}$, $s_{ij} \equiv \sin\theta_{ij}$, and $\phi_{12}, \phi_{13}, \phi_{23}$ are the physical phases.

The mixing angles in terms of the $\mathbf{U}_{\mathrm{PMNS}}$ matrix entries are

$$\sin^2\theta_{12} = \frac{|U_{e2}|^2}{1-|U_{e3}|^2}, \quad \sin^2\theta_{23} = \frac{|U_{\mu 3}|^2}{1-|U_{e3}|^2},$$
$$\sin^2\theta_{13} = |U_{e3}|^2. \tag{6}$$

Whereas, the phase factors associated with the CP violation phases are:

$$\sin\delta_{\mathrm{CP}} = \frac{\mathcal{J}_{\mathrm{CP}}\left(1-|U_{e3}|^2\right)}{|U_{e1}||U_{e2}||U_{e3}||U_{\mu 3}||U_{\tau 3}|},$$
$$\sin\left(-2\phi_{12}\right) = \frac{\mathcal{I}_1}{|U_{e1}|^2|U_{e2}|^2},$$
$$\sin\left(-2\phi_{13}\right) = \frac{\mathcal{I}_2}{|U_{e1}|^2|U_{e3}|^2}. \tag{7}$$

$\mathcal{J}_{\mathrm{CP}} = \mathbb{I}m\left\{U_{e3}U^*_{\mu 3}U^*_{e1}U_{\mu 1}\right\}$ is the Jarlskog invariant, which is associated with the Dirac-like CP violation phase,

$$\mathcal{I}_1 = \mathbb{I}m\left\{|U_{e1}|^2|U_{e2}|^2\right\} \quad \text{and} \quad \mathcal{I}_2 = \mathbb{I}m\left\{|U_{e1}|^2|U_{e3}|^2\right\},$$

which are the invariants associated with the CP violation phase factors Majorana-like.

2. The TBM leptonic flavor pattern

In the theoretical framework of TBM flavor mixing pattern, the charged lepton mass matrix has a diagonal form $\mathrm{diag}\left(m_e, m_\mu, m_\tau\right)$, while, the solar, atmospheric and reactor mixing angles have the values

$$\sin^2\theta_{12} = \frac{1}{2}, \quad \theta_{23} = \frac{\pi}{4}, \quad \theta_{13} = 0. \tag{8}$$

The CP symmetry is preserved, this means that phase factors are null.

The unitary matrix $\mathbf{U}_\ell$ is equal to identity matrix, and $\mathbf{U}_{\mathrm{TBM}} = \mathbf{U}_{\mathrm{PMNS}} = \mathbf{U}_\nu$ is expressed as

$$\mathbf{U}_{\mathrm{TBM}} = \begin{pmatrix} \sqrt{\frac{2}{3}} & \frac{1}{\sqrt{3}} & 0 \\ -\frac{1}{\sqrt{6}} & \frac{1}{\sqrt{3}} & \frac{1}{\sqrt{2}} \\ \frac{1}{\sqrt{6}} & -\frac{1}{\sqrt{3}} & \frac{1}{\sqrt{2}} \end{pmatrix}. \tag{9}$$

So, the neutrino mass matrix has the form

$$\mathbf{M}_\nu = \begin{pmatrix} b_\nu & a_\nu & -a_\nu \\ a_\nu & b_\nu + d_\nu & b_\nu + c_\nu \\ -a_\nu & b_\nu + c_\nu & b_\nu + d_\nu \end{pmatrix}, \tag{10}$$

where

$$a_\nu = \frac{1}{3}\left(m_{\nu 2} - m_{\nu 1}\right), \quad c_\nu = \frac{1}{2}\left(m_{\nu 3} - \frac{4}{3}m_{\nu 2} - \frac{5}{3}m_{\nu 1}\right),$$
$$b_\nu = \frac{1}{3}\left(2m_{\nu 1} + m_{\nu 2}\right), \quad d_\nu = \frac{1}{2}\left(m_{\nu 3} - m_{\nu 1}\right).$$

Unfortunately, the TBM leptonic flavor pattern does not work to describe the nature, since the reactor mixing angle is non null, by according with the current experimental data on neutrino oscillations [6]:

$$\sin^2\theta_{12}\left(10^{-1}\right)=3.18\pm0.16,\quad 2.71-3.69,$$

$$\sin^2\theta_{23}\left(10^{-1}\right)=\begin{cases}5.74\pm0.14, & 4.34-6.10, & \text{for NH},\\ 5.78^{+0.10}_{-0.17}, & 4.33-6.08, & \text{for IH},\end{cases}$$

$$\sin^2\theta_{13}\left(10^{-2}\right)=\begin{cases}2.200^{+0.069}_{-0.062}, & 2.000-2.405 & \text{for NH},\\ 2.225^{+0.064}_{-0.070}, & 2.018-2.424 & \text{for IH}.\end{cases}$$

3. Deviations from the TBM flavor pattern

A possible modification to the TBM flavor pattern may come from the charged lepton sector considering a non-diagonal leptonic mass matrix $\mathbf{M}_\ell$.

In order to fix the form of the charged lepton mass matrix, we propose several equivalence classes whose elements are Hermitian matrices with two texture zeros given by

$$\mathbf{M}_\ell^i=\mathbf{U}_\ell^i\mathbf{\Delta}_\ell\mathbf{U}_\ell^{i\dagger}. \tag{11}$$

Here,

$$\mathbf{U}_\ell^i=\mathbf{T}_i\mathbf{P}_\ell^\dagger\mathbf{O}_\ell,\qquad i=0,...,5\,, \tag{12}$$

where the $\mathbf{T}_i$ are the elements of S_3 real representation, $\mathbf{P}_\ell$ is the diagonal matrix of phase factors, and $\mathbf{O}_\ell$ is a real orthogonal matrix (see Appendix A in Ref. [20]). The PMNS mixing matrix takes the form

$$\mathbf{U}^i_{\rm PMNS}=\mathbf{U}_\ell^{i\dagger}\mathbf{U}_\nu=\mathbf{O}_\ell^\top\mathbf{P}_\ell\mathbf{T}_i\mathbf{U}_{\rm TBM}. \tag{13}$$

The explicit form of the $\mathbf{O}_\ell$ and $\mathbf{P}_\ell$ matrices depends on the equivalence class.

3.1. Equivalent classes with two texture zeros

The rule under which texture zeros in a matrix are counted is; one texture-zero on the diagonal counts as one, while two off-diagonal counts as one texture zero. Then, we shown the four equivalent class kinds with two texture zeros.

Hermitian matrices Type-I

$$\begin{aligned}
\mathbf{M}_\ell^0&=\begin{pmatrix}0&a_\ell&0\\a_\ell^*&b_\ell&c_\ell\\0&c_\ell^*&d_\ell\end{pmatrix},\quad \mathbf{M}_\ell^1=\begin{pmatrix}b_\ell&a_\ell^*&c_\ell\\a_\ell&0&0\\c_\ell^*&0&d_\ell\end{pmatrix},\quad \mathbf{M}_\ell^2=\begin{pmatrix}d_\ell&c_\ell^*&0\\c_\ell&b_\ell&a_\ell^*\\0&a_\ell&0\end{pmatrix},\\
\mathbf{M}_\ell^3&=\begin{pmatrix}0&0&a_\ell\\0&d_\ell&c_\ell^*\\a_\ell^*&c_\ell&b_\ell\end{pmatrix},\quad \mathbf{M}_\ell^4=\begin{pmatrix}d_\ell&0&c_\ell^*\\0&0&a_\ell\\c_\ell&a_\ell^*&b_\ell\end{pmatrix},\quad \mathbf{M}_\ell^5=\begin{pmatrix}b_\ell&c_\ell&a_\ell^*\\c_\ell^*&d_\ell&0\\a_\ell&0&0\end{pmatrix},
\end{aligned} \tag{14}$$

Hermitian matrices Type-II

$$\begin{aligned}
\mathbf{M}_\ell^0&=\begin{pmatrix}f_\ell&a_\ell&0\\a_\ell^*&0&c_\ell\\0&c_\ell^*&d_\ell\end{pmatrix},\quad \mathbf{M}_\ell^1=\begin{pmatrix}0&a_\ell^*&c_\ell\\a_\ell&f_\ell&0\\c_\ell^*&0&d_\ell\end{pmatrix},\quad \mathbf{M}_\ell^2=\begin{pmatrix}d_\ell&c_\ell^*&0\\c_\ell&0&a_\ell^*\\0&a_\ell&f_\ell\end{pmatrix},\\
\mathbf{M}_\ell^3&=\begin{pmatrix}f_\ell&0&a_\ell\\0&d_\ell&c_\ell^*\\a_\ell^*&c_\ell&0\end{pmatrix},\quad \mathbf{M}_\ell^4=\begin{pmatrix}d_\ell&0&c_\ell^*\\0&f_\ell&a_\ell\\c_\ell&a_\ell^*&0\end{pmatrix},\quad \mathbf{M}_\ell^5=\begin{pmatrix}0&c_\ell&a_\ell^*\\c_\ell^*&d_\ell&0\\a_\ell&0&f_\ell\end{pmatrix},
\end{aligned} \tag{15}$$

Hermitian matrices Type-III

$$\begin{aligned}
\mathbf{M}_\ell^0&=\begin{pmatrix}0&a_\ell&e_\ell\\a_\ell^*&0&c_\ell\\e_\ell^*&c_\ell^*&d_\ell\end{pmatrix},\quad \mathbf{M}_\ell^1=\begin{pmatrix}0&a_\ell^*&c_\ell\\a_\ell&0&e_\ell\\c_\ell^*&e_\ell^*&d_\ell\end{pmatrix},\quad \mathbf{M}_\ell^2=\begin{pmatrix}d_\ell&c_\ell^*&e_\ell^*\\c_\ell&0&a_\ell^*\\e_\ell&a_\ell&0\end{pmatrix},\\
\mathbf{M}_\ell^3&=\begin{pmatrix}0&e_\ell&a_\ell\\e_\ell^*&d_\ell&c_\ell^*\\a_\ell^*&c_\ell&0\end{pmatrix},\quad \mathbf{M}_\ell^4=\begin{pmatrix}d_\ell&e_\ell^*&c_\ell^*\\e_\ell&0&a_\ell\\c_\ell&a_\ell^*&0\end{pmatrix},\quad \mathbf{M}_\ell^5=\begin{pmatrix}0&c_\ell&a_\ell^*\\c_\ell^*&d_\ell&e_\ell^*\\a_\ell&e_\ell&0\end{pmatrix},
\end{aligned} \tag{16}$$

Hermitian matrices Type-IV

$$\mathbf{M}_\ell^0=\begin{pmatrix} f_\ell & a_\ell & 0\\ a_\ell^* & b_\ell & 0\\ 0 & 0 & d_\ell\end{pmatrix},\quad \mathbf{M}_\ell^1=\begin{pmatrix} b_\ell & a_\ell & 0\\ a_\ell^* & f_\ell & 0\\ 0 & 0 & d_\ell\end{pmatrix},\quad \mathbf{M}_\ell^2=\begin{pmatrix} d_\ell & 0 & 0\\ 0 & b_\ell & a_\ell^*\\ 0 & a_\ell & f_\ell\end{pmatrix},$$
$$\mathbf{M}_\ell^3=\begin{pmatrix} f_\ell & 0 & a_\ell\\ 0 & d_\ell & 0\\ a_\ell^* & 0 & b_\ell\end{pmatrix},\quad \mathbf{M}_\ell^4=\begin{pmatrix} d_\ell & 0 & 0\\ 0 & f_\ell & a_\ell\\ 0 & a_\ell^* & b_\ell\end{pmatrix},\quad \mathbf{M}_\ell^5=\begin{pmatrix} b_\ell & 0 & a_\ell^*\\ 0 & d_\ell & 0\\ a_\ell & 0 & f_\ell\end{pmatrix}, \tag{17}$$

In this paper, to analyze the feasibility of the textures, and one of the equivalent class, here we only present the analysis for the equivalence class with two zeroes texture type-I. The others are developed in Ref. [13].

4. Equivalent class with two texture zeros type-I

To analyze the deviation from the TBM pattern, we focus on the Hermitian matrices with two texture zeros type-I Eq. (14). By considering Eq. (14) and using the matrix invariants

$$\mathrm{Tr}\left\{\mathbf{M}_\ell^i\right\},\qquad \mathrm{Det}\left\{\mathbf{M}_\ell^i\right\},$$
$$\chi\left\{\mathbf{M}_\ell^i\right\}=\frac{1}{2}\left(\mathrm{Tr}\left\{\mathbf{M}_\ell^{i2}\right\}-\mathrm{Tr}\left\{\mathbf{M}_\ell^i\right\}^2\right),$$

the mass matrices elements in terms of charged lepton masses, δ_ℓ, ϕ_a and ϕ_c parameters have the form $d_\ell=1-\delta_\ell$,

$$a_\ell=\sqrt{\frac{\widetilde{m}_e\widetilde{m}_\mu}{1-\delta_\ell}}\,e^{i\phi_a},$$
$$b_\ell=(\mathsf{s}_3-1)+\mathsf{s}_1\widetilde{m}_e+\mathsf{s}_2\widetilde{m}_\mu+\delta_\ell,$$
$$c_\ell=\sqrt{\frac{f_{\ell1}f_{\ell2}f_{\ell3}}{1-\delta_\ell}}\,e^{i\phi_c},$$

being δ_ℓ such that $0<\delta_\ell<1$, with

$$f_{\ell1}=1-\mathsf{s}_1\widetilde{m}_e-\delta_\ell,$$
$$f_{\ell2}=\mathsf{s}_3\left(1-\mathsf{s}_2\widetilde{m}_\mu-\delta_\ell\right),$$
$$f_{\ell3}=1+\mathsf{s}_3\left(\delta_\ell-1\right).$$

$\widetilde{m}_e=m_e/m_\tau$, and $\widetilde{m}_\mu=m_\mu/m_\tau$; $\phi_a=\arg\{a_\ell\}$, and $\phi_c=\arg\{c_\ell\}$ are related to the CP violation and are defined in the interval $(-\pi,\pi]$. $\mathsf{s}_k=\mathrm{sign}\left(m_{\ell k}\right)$ with $k=1,2,3$. For charged lepton fields the sign of the mass is irrelevant since the sign can be changed by means of the chiral transformations,

$$\ell_R\to\ell'_R=e^{i\gamma_5\frac{\pi}{2}}\ell_R,\quad \text{and}\quad \ell_L\to\ell'_L=e^{i\gamma_5\frac{\pi}{2}}\ell_L.$$

These transformations change the sign of the eigenvalues, however, the rest of the Lagrangian keeps invariant.

The parameter δ_ℓ must satisfy the following conditions:

A. $0<\delta_\ell<1-\widetilde{m}_\mu,\quad$ for $\quad m_e{=}-\mid m_e\mid$.

B. $0<\delta_\ell<1-\widetilde{m}_e,\ \delta_\ell\neq\widetilde{m}_\mu-\widetilde{m}_e,\quad$ for $\quad m_\mu{=}-\mid m_\mu\mid$.

C. $1-\widetilde{m}_\mu<\delta_\ell<1-\widetilde{m}_e,\quad$ for $\quad m_\tau{=}-\mid m_\tau\mid$.

In the above, the minus sign means which chiral rotation we apply. Considering the previous results, the PMNS matrix takes the form $\mathbf{U}^i_{\mathrm{PMNS}}=\mathbf{O}_\ell^\top\mathbf{P}_\ell\mathbf{T}_i\mathbf{U}_{\mathrm{TBM}}$, where

$$\mathbf{O}_\ell=\begin{pmatrix} \mathsf{s}_1\sqrt{\frac{\widetilde{m}_\mu f_{\ell1}}{D_{\ell1}}} & \mathsf{s}_2\sqrt{\frac{\widetilde{m}_e f_{\ell2}}{D_{\ell2}}} & \mathsf{s}_3\sqrt{\frac{\widetilde{m}_e\widetilde{m}_\mu f_{\ell3}}{D_{\ell3}}}\\ \sqrt{\frac{\widetilde{m}_e(1-\delta_\ell)f_{\ell1}}{D_{\ell1}}} & \sqrt{\frac{\widetilde{m}_\mu(1-\delta_\ell)f_{\ell2}}{D_{\ell2}}} & \sqrt{\frac{(1-\delta_\ell)f_{\ell3}}{D_{\ell3}}}\\ -\sqrt{\frac{\widetilde{m}_e f_{\ell2}f_{\ell3}}{D_{\ell1}}} & \mathsf{s}_1\mathsf{s}_2\sqrt{\frac{\widetilde{m}_\mu f_{\ell1}f_{\ell3}}{D_{\ell2}}} & \mathsf{s}_3\sqrt{\frac{f_{\ell1}f_{\ell2}}{D_{\ell3}}}\end{pmatrix},$$

where

$$D_{\ell1}=(1-\delta_\ell)\left(\widetilde{m}_\mu+\mathsf{s}_3\widetilde{m}_e\right)\left(1+\mathsf{s}_2\widetilde{m}_e\right),$$
$$D_{\ell2}=(1-\delta_\ell)\left(\widetilde{m}_\mu+\mathsf{s}_3\widetilde{m}_e\right)\left(1+\mathsf{s}_1\widetilde{m}_\mu\right),$$
$$D_{\ell3}=(1-\delta_\ell)\left(1+\mathsf{s}_2\widetilde{m}_e\right)\left(1+\mathsf{s}_1\widetilde{m}_\mu\right). \tag{18}$$

In this case, the flavor mixing angles can be expressed as

$$\sin^2\theta_{12}=\frac{1}{3}\frac{\widetilde{m}_e}{\widetilde{m}_\mu}\varepsilon_{12}, \tag{19}$$

$$\sin^2\theta_{23}=\frac{1}{2}\frac{(1+\mathsf{s}_2\widetilde{m}_e)}{(1+\mathsf{s}_1\widetilde{m}_\mu)}\varepsilon_{23}, \tag{20}$$

$$\sin^2\theta_{13}=\frac{1}{2}\frac{\widetilde{m}_e}{\widetilde{m}_\mu}\varepsilon_{13}. \tag{21}$$

The explicit form of the ε_{ij} parameters depends on the shape of charged lepton mass matrix, explicit expressions for equivalent class type-I are given in Appendix A (see the others types in Ref. [13]). The matrices $\mathbf{M}_\ell^0$ and $\mathbf{M}_\ell^3$ ($\mathbf{M}_\ell^1$ and $\mathbf{M}_\ell^5$; $\mathbf{M}_\ell^2$ and $\mathbf{M}_\ell^4$) generate the same form for the ε_{12}, ε_{23}, and ε_{13} parameters.

5. Numerical analysis

This section contains the numerical analysis of the allowed regions for the reactor, atmospheric and solar mixing angles, see Ref. [13].

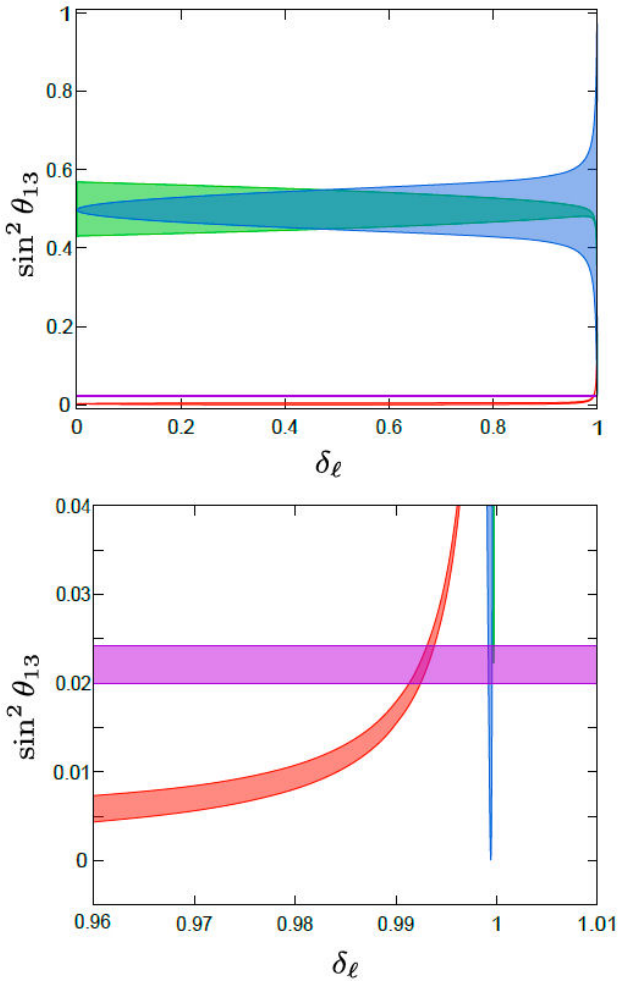

FIGURE 1. The allowed regions for the reactor mixing angle θ_{13} & δ_ℓ for equivalent class with two texture zeros type-I. The purple stripe corresponds to the values at 3σ for the reactor mixing angle obtained from the global fit, for normal and inverted hierarchy [6]. In these panels, the red area is for $\mathbf{M}_\ell^0$ and $\mathbf{M}_\ell^3$, blue area is for $\mathbf{M}_\ell^1$ and $\mathbf{M}_\ell^5$, the green area is for an$\mathbf{M}_\ell^2$ and $\mathbf{M}_\ell^4$. In the lower panel shows an amplification of the region in which the mixing angle theoretical expressions simultaneously reproduce the current experimental data.

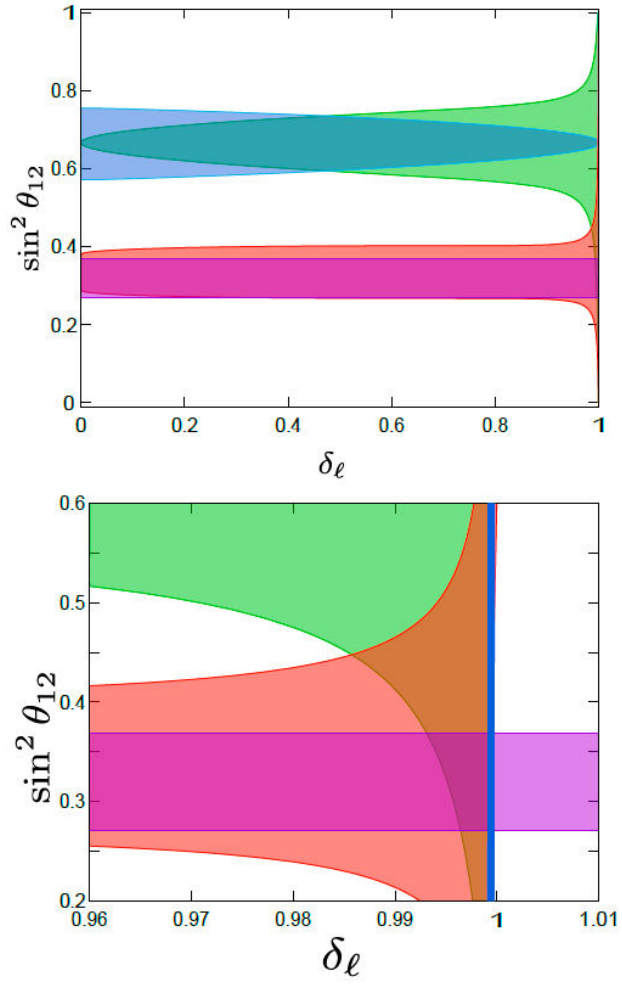

FIGURE 2. The allowed regions for the solar mixing angle θ_{12} & δ_ℓ, for equivalent class with two texture zeros type-I. Remaining information as in Fig. 1.

It is easy to conclude that all charged lepton mass matrices are able to reproduce the current experimental values of reactor mixing angle. However, the numerical values interval of the free parameter δ_ℓ, for the $\mathbf{M}_\ell^1$, $\mathbf{M}_\ell^2$, $\mathbf{M}_\ell^4$ and $\mathbf{M}_\ell^5$ mass matrices, is too small.

In Figs. 1, 2, and 3, the purple stripe corresponds to the values at 3σ for reactor mixing angle θ_{13}, solar mixing angle θ_{12}, and atmospheric mixing angle θ_{23} respectively, obtained from the global fit, for normal and inverted hierarchy. In these panels, the red area is for $\mathbf{M}_\ell^0$ and $\mathbf{M}_\ell^3$, and the green area is for $\mathbf{M}_\ell^2$ and $\mathbf{M}_\ell^4$. In each figure, the lower panel shows an amplification of the region in which the mixing angles theoretical expressions simultaneously reproduce the current experimental data.

The free parameter δ_ℓ should be in the following numerical interval:

$$\begin{aligned} \delta_\ell &\in [0.99132, 0.99382] \quad \text{for} \quad \mathbf{M}_\ell^0 \quad \text{and} \quad \mathbf{M}_\ell^3, \\ \delta_\ell &\approx 0.9994 \quad \text{for} \quad \mathbf{M}_\ell^1 \quad \text{and} \quad \mathbf{M}_\ell^5, \\ \delta_\ell &\approx 0.9997 \quad \text{for} \quad \mathbf{M}_\ell^2 \quad \text{and} \quad \mathbf{M}_\ell^4, \end{aligned}$$

whereas for the phase factors,

$$\begin{aligned} |\phi_a| &\in [76^\circ, 180^\circ] \quad \text{for} \quad \mathbf{M}_\ell^2,\ \mathbf{M}_\ell^4, \\ |\phi_c| &\in [76^\circ, 180^\circ] \quad \text{for} \quad \mathbf{M}_\ell^0,\ \mathbf{M}_\ell^3. \end{aligned}$$

5.1. Neutrinoless double-beta decay

The neutrinoless double beta decay $(0\nu\beta\beta)$ is a second-order process in which a nucleus decays into another by the emission of two electrons

$$(A, Z) \to (A, Z+2) + e^- + e^-.$$

The experimental discovery of one of these processes could solve the open question about particles, which means that it

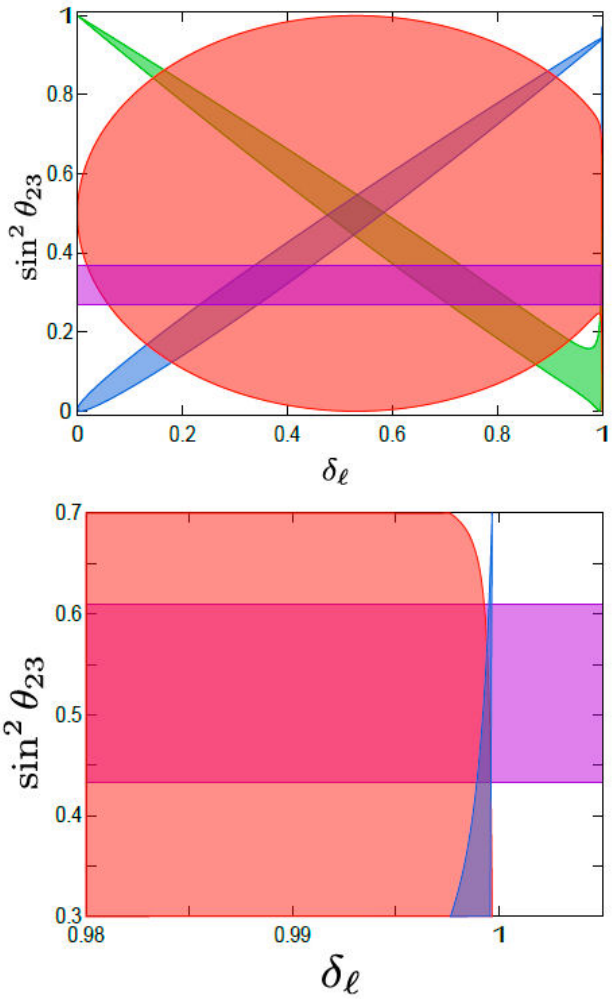

FIGURE 3. The allowed regions for the atmospheric mixing angles θ_{23} & δ_ℓ, for equivalent class with two texture zeros type-I and type-III. Remaining information as in Fig. 1.

would be the first signal of the non-conservation of the lepton number. The amplitude for $(0\nu\beta\beta)$ is proportional to the Majorana effective mass

$$m_{ee} = \sum_i m_{\nu_i} U_{ei}^2, \quad i = 1, 2, 3,$$

where m_{ν_i} $(i = 1, 2, 3)$ are the Majorana neutrino masses and U_{ei} the elements of the first row of leptonic flavor mixing matrix PMNS.

In the symmetric parametrization of leptonic flavor mixing matrix, the Majorana effective mass has the form

$$|m_{ee}| = |m_{\nu_1} c_{12}^2 c_{13}^2 + m_{\nu_2} s_{12}^2 c_{13}^2 e^{-i2\phi_{12}} + m_{\nu_3} s_{13}^2 e^{-i2\phi_{13}}|,$$

where ϕ_{12} and ϕ_{13} are the Majorana phase factor.

The m_{ν_i} neutrino masses can be written in terms of the lightest neutrino mass through the expressions

$$m_{\nu_{3[2]}} = \sqrt{m_{\nu_{1[3]}} + \Delta m^2_{31[23]}},$$

$$m_{\nu_{2[1]}} = \sqrt{m_{\nu_{1[3]}} + \Delta m^2_{21[31]}},$$

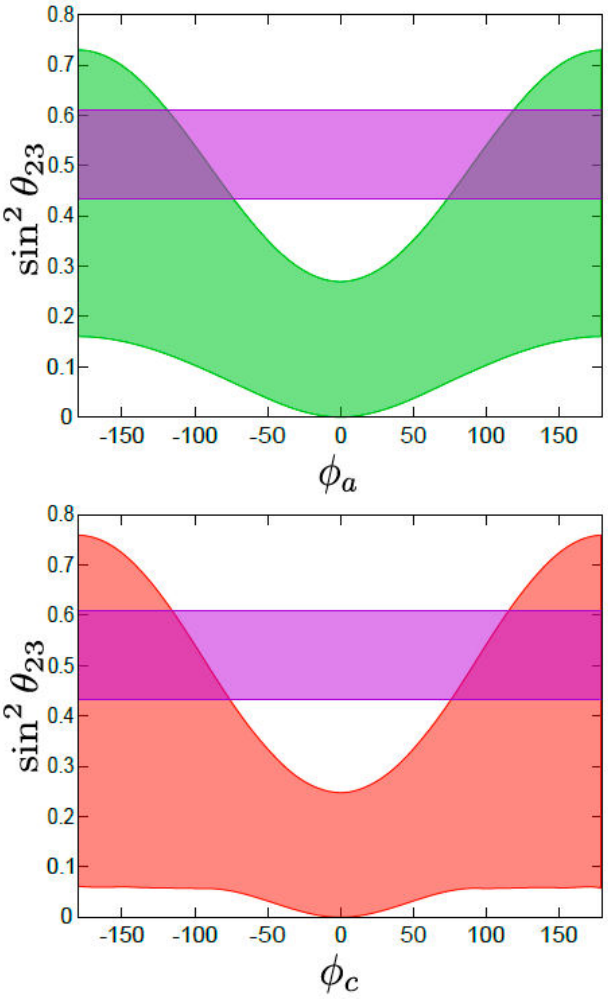

FIGURE 4. The allowed regions for the atmospheric mixing angle θ_{23} & ϕ_a, ϕ_c, for equivalent class with two texture zeros type-I.

where the $\Delta m^2_{ij} = m^2_{\nu_i} - m^2_{\nu_j}$ and $m_{\nu_{1[3]}}$ is the lightest neutrino mass for the normal[inverted] hierarchy in the neutrino mass spectrum.

Figure 4 shows the allowed regions for the atmospheric mixing angle θ_{23} as function of ϕ_a (upper panel) and ϕ_c (lower panel).

In the upper panel, the red area is for a normal hierarchy while the orange area is normal hierarchy, both areas are obtained from matrices $\mathbf{M}_\ell^0$ and $\mathbf{M}_\ell^3$. In the middle panel, the magenta area is hierarchy while the blue area is for an inverted hierarchy, both areas are obtained from $\mathbf{M}_\ell^1$ and $\mathbf{M}_\ell^5$. Finally, in the lower panel, the green area is for a normal hierarchy while the cyan area is for an inverted hierarchy, both areas are obtained from $\mathbf{M}_\ell^2$ and $\mathbf{M}_\ell^4$. From KamLAND-ZEN and EXO-200, the following upper limit $m_{ee} < 0.061$, which correspond to the horizontal gray band. From the results reported by Planck collaboration, obtaining the vertical gray band.

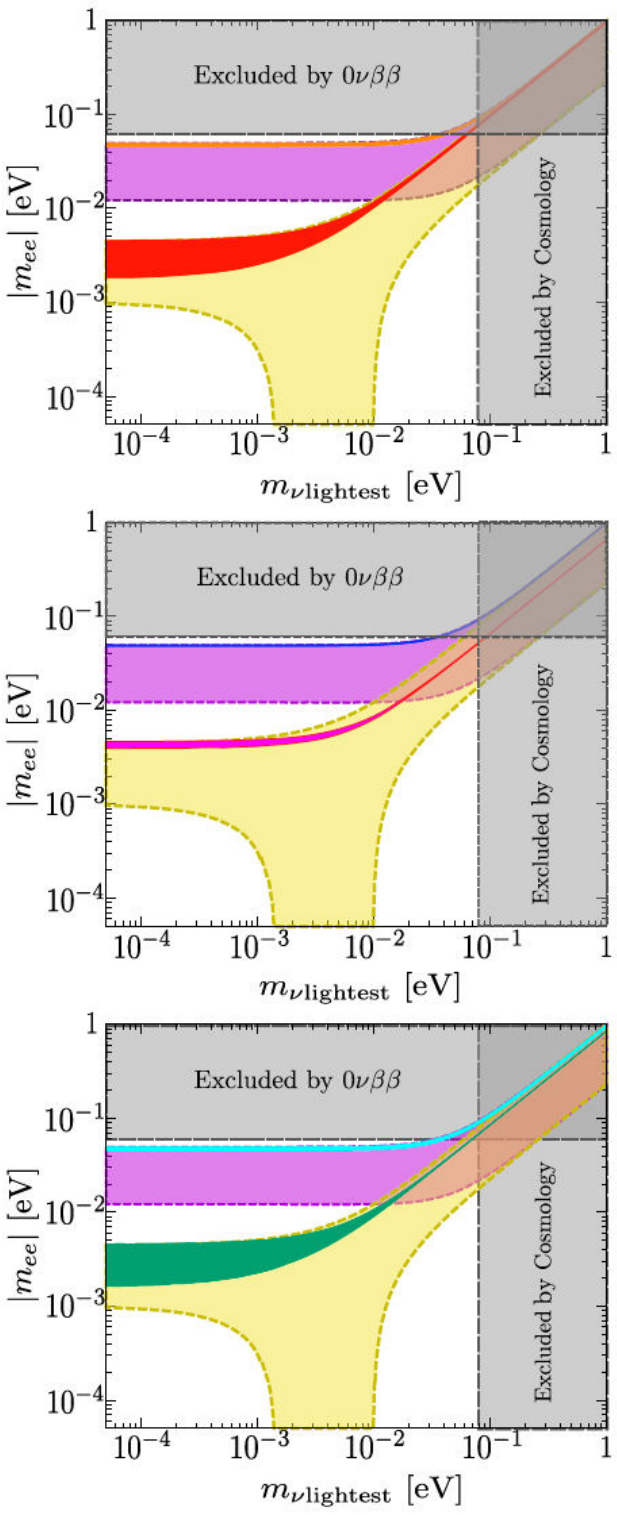

FIGURE 5. In these panels, regions allowed for the magnitude of Majorana effective mass $|m_{ee}|$ are shown.

In Fig. 5, $|m_{ee}|$ & $m_{\nu ligntest}$ are shown for an inverted and normal neutrino mass hierarchy, the yellow and purple stripes are obtained from the current experimental data on neutrino oscillations at 3σ [6].

6. Summary

In a model-independent theoretical framework, we presented a generalization of TBM leptonic flavor mixing pattern. In this modification to the TBM pattern, the unitary matrix that diagonalizes to the neutrino mass matrix is represented by means of TBM flavor mixing pattern, whereas the charged lepton mass matrix is represented by one of the elements of the equivalence classes with two texture zeros. Particularly, we shown a deviation from the TBM pattern in terms of the charged lepton masses as well as the theoretical expressions and their parameter space for the mixing angles. Furthermore, from the theoretical expressions of ε_{ij} in Appendix A we have for each type of equivalent class the $\mathbf{M}_\ell^0$ and $\mathbf{M}_\ell^3$ matrices generate the same expressions for ϵ_{23} and ϵ_{13}; similarly for $\mathbf{M}_\ell^2$ and $\mathbf{M}_\ell^4$, as well as $\mathbf{M}_\ell^1$ and $\mathbf{M}_\ell^5$.

From the analysis performed for equivalence classes type-I, we had that it is easy to conclude that all charged lepton mass matrices $\mathbf{M}_\ell^i$ ($i = 0, \ldots, 5$) are able to reproduce the current experimental values of reactor, solar and atmospheric angles. But, the numerical interval of the free parameter δ_ℓ, for the $\mathbf{M}_\ell^1$, $\mathbf{M}_\ell^2$, $\mathbf{M}_\ell^4$ and $\mathbf{M}_\ell^5$, is too small,

$$\begin{aligned} \delta_\ell &\in [0.99132, 0.99382] \quad \text{for} \quad \mathbf{M}_\ell^0 \quad \text{and} \quad \mathbf{M}_\ell^3, \\ \delta_\ell &\approx 0.9994 \quad \text{for} \quad \mathbf{M}_\ell^1 \quad \text{and} \quad \mathbf{M}_\ell^5, \\ \delta_\ell &\approx 0.9997 \quad \text{for} \quad \mathbf{M}_\ell^2 \quad \text{and} \quad \mathbf{M}_\ell^4. \end{aligned}$$

On the other hand, for all mass matrices $\mathbf{M}_\ell^i$ ($i = 0, \ldots, 5$), the solar and reactor mixing angles have a weak dependence on phases ϕ_a and ϕ_c; whereas for $\mathbf{M}_\ell^1$ and $\mathbf{M}_\ell^5$, the atmospheric mixing angle has a weak dependence on ϕ_a and ϕ_c.

However, to reproduce the current experimental data for the mixing angle θ_{23}, for $\mathbf{M}_\ell^0$ and $\mathbf{M}_\ell^3$ ($\mathbf{M}_\ell^2$ and $\mathbf{M}_\ell^4$), the phase ϕ_c (ϕ_a) runs over the numerical range

$$\begin{aligned} |\phi_a| &\in [76^\circ, 180^\circ] \quad \text{for} \quad \mathbf{M}_\ell^2 \quad \text{and} \quad \mathbf{M}_\ell^4, \\ |\phi_c| &\in [76^\circ, 180^\circ] \quad \text{for} \quad \mathbf{M}_\ell^0 \quad \text{and} \quad \mathbf{M}_\ell^3. \end{aligned}$$

Appendix

A. Parameters of equivalent class with two texture zeros type-I

For the mass matrices $\mathbf{M}_\ell^0$ and $\mathbf{M}_\ell^3$,

$$\varepsilon_{23} = \frac{(1+\mathtt{s}_3(\delta_\ell-1))f_{\ell1}+(1-\delta_\ell)f_{\ell2}+\mathtt{s}_1\mathtt{s}_2 2\sqrt{(1+\mathtt{s}_3(\delta_\ell-1))(1-\delta_\ell)f_{\ell1}f_{\ell2}}\cos\phi_c}{(1-\delta_\ell)\left(1+\mathtt{s}_3\frac{\widetilde{m}_e}{\widetilde{m}_\mu}\right)(1+\mathtt{s}_2\widetilde{m}_e)+\frac{1}{2}\frac{\widetilde{m}_e}{\widetilde{m}_\mu}\left(f_{\ell2}(1+\mathtt{s}_3(\delta_\ell-1))+f_{\ell1}(1-\delta_\ell)-2\sqrt{(1+\mathtt{s}_3(\delta_\ell-1))(1-\delta_\ell)f_{\ell1}f_{\ell2}}\cos\phi_c\right)},$$

$$\varepsilon_{13} = \frac{f_{\ell2}(1+\mathtt{s}_3(\delta_\ell-1))+f_{\ell1}(1-\delta_\ell)-2\sqrt{(1-\delta_\ell)(1+\mathtt{s}_3(\delta_\ell-1))f_{\ell1}f_{\ell2}}\cos\phi_c}{(1-\delta_\ell)\left(1+\mathtt{s}_3\frac{\widetilde{m}_e}{\widetilde{m}_\mu}\right)(1+\mathtt{s}_2\widetilde{m}_e)},$$

$$\varepsilon_{12} = \frac{f_{\ell2}(1+\mathtt{s}_3(\delta_\ell-1))+f_{\ell1}\frac{\widetilde{m}_\mu}{\widetilde{m}_e}+f_{\ell1}(1-\delta_\ell)+2\sqrt{(1+\mathtt{s}_3(\delta_\ell-1))(1-\delta_\ell)f_{\ell1}f_{\ell2}}c_c+(-1)^i\mathtt{s}_1 2\left(\sqrt{\frac{\widetilde{m}_\mu}{\widetilde{m}_e}(1+\mathtt{s}_3(\delta_\ell-1))f_{\ell1}f_{\ell2}}c_{ac}+f_{\ell1}\sqrt{\frac{\widetilde{m}_\mu}{\widetilde{m}_e}(1-\delta_\ell)}c_a\right)}{(1-\delta_\ell)\left(1+\mathtt{s}_3\frac{\widetilde{m}_e}{\widetilde{m}_\mu}\right)(1+\mathtt{s}_2\widetilde{m}_e)-\frac{1}{2}\frac{\widetilde{m}_e}{\widetilde{m}_\mu}f_{\ell2}(1+\mathtt{s}_3(\delta_\ell-1))+(1-\delta_\ell)f_{\ell1}-2\sqrt{(1-\delta_\ell)(1+\mathtt{s}_3(\delta_\ell-1))f_{\ell1}f_{\ell2}}c_c},$$

(A.1)

where $i=0$ for $\mathbf{M}^0_\ell$, $i=1$ for $\mathbf{M}^3_\ell$, $c_a \equiv \cos\phi_a$, $c_c \equiv \cos\phi_c$, and $c_{ac} \equiv \cos(\phi_a+\phi_c)$.

For $\mathbf{M}^1_\ell$ and $\mathbf{M}^5_\ell$:

$$\varepsilon_{23} = \frac{\frac{\widetilde{m}_e}{\widetilde{m}_\mu}f_{\ell2}+(1+\mathtt{s}_3(\delta_\ell-1))f_{\ell1}+\mathtt{s}_1 2\sqrt{\frac{\widetilde{m}_e}{\widetilde{m}_\mu}(1+\mathtt{s}_3(\delta_\ell-1))f_{\ell1}f_{\ell2}}\cos(\phi_a+\phi_c)}{(1-\delta_\ell)\left(1+\mathtt{s}_3\frac{\widetilde{m}_e}{\widetilde{m}_\mu}\right)(1+\mathtt{s}_2\widetilde{m}_e)-\frac{1}{2}\frac{\widetilde{m}_e}{\widetilde{m}_\mu}\left(f_{\ell2}(1+\mathtt{s}_3(\delta_\ell-1))+\frac{\widetilde{m}_\mu}{\widetilde{m}_e}f_{\ell1}-\mathtt{s}_1 2\sqrt{\frac{\widetilde{m}_\mu}{\widetilde{m}_e}(1+\mathtt{s}_3(\delta_\ell-1))f_{\ell1}f_{\ell2}}\cos(\phi_a+\phi_c)\right)},$$

$$\varepsilon_{13} = \frac{f_{\ell2}(1+\mathtt{s}_3(\delta_\ell-1))+\frac{\widetilde{m}_\mu}{\widetilde{m}_e}f_{\ell1}-\mathtt{s}_1 2\sqrt{\frac{\widetilde{m}_\mu}{\widetilde{m}_e}(1+\mathtt{s}_3(\delta_\ell-1))f_{\ell1}f_{\ell2}}\cos(\phi_a+\phi_c)}{(1-\delta_\ell)\left(1+\mathtt{s}_3\frac{\widetilde{m}_e}{\widetilde{m}_\mu}\right)(1+\mathtt{s}_2\widetilde{m}_e)},$$

$$\varepsilon_{12} = \frac{f_{\ell2}(1+\mathtt{s}_3(\delta_\ell-1))+f_{\ell1}\frac{\widetilde{m}_\mu}{\widetilde{m}_e}+f_{\ell1}(1-\delta_\ell)+2\mathtt{s}_1\sqrt{\frac{\widetilde{m}_\mu}{\widetilde{m}_e}(1+\mathtt{s}_3(\delta_\ell-1))f_{\ell1}f_{\ell2}}c_{ac}+(-1)^i 2\left(\sqrt{(1+\mathtt{s}_3(\delta_\ell-1))(1-\delta_\ell)f_{\ell1}f_{\ell2}}c_c+\mathtt{s}_1 f_{\ell1}\sqrt{\frac{\widetilde{m}_\mu}{\widetilde{m}_e}(1-\delta_\ell)}c_a\right)}{(1-\delta_\ell)\left(1+\mathtt{s}_3\frac{\widetilde{m}_e}{\widetilde{m}_\mu}\right)(1+\mathtt{s}_2\widetilde{m}_e)-\frac{1}{2}\frac{\widetilde{m}_e}{\widetilde{m}_\mu}f_{\ell2}(1+\mathtt{s}_3(\delta_\ell-1))+f_{\ell1}\frac{\widetilde{m}_\mu}{\widetilde{m}_e}-2\mathtt{s}_1\sqrt{\frac{\widetilde{m}_\mu}{\widetilde{m}_e}(1+\mathtt{s}_3(\delta_\ell-1))f_{\ell1}f_{\ell2}}c_{ac}},$$

(A.2)

where $i=0$ for $\mathbf{M}^1_\ell$, $i=1$ for $\mathbf{M}^5_\ell$.

For $\mathbf{M}^2_\ell$ and $\mathbf{M}^4_\ell$,

$$\varepsilon_{23} = \frac{f_{\ell2}\left(1-\delta_\ell+\frac{\widetilde{m}_e}{\widetilde{m}_\mu}+\mathtt{s}_2 2\sqrt{\frac{\widetilde{m}_e}{\widetilde{m}_\mu}(1-\delta_\ell)}\cos\phi_a\right)}{(1-\delta_\ell)\left(1+\mathtt{s}_3\frac{\widetilde{m}_e}{\widetilde{m}_\mu}\right)(1+\mathtt{s}_2\widetilde{m}_e)-\frac{1}{2}\frac{\widetilde{m}_e}{\widetilde{m}_\mu}f_{\ell1}\left(1-\delta_\ell+\frac{\widetilde{m}_\mu}{\widetilde{m}_e}+\mathtt{s}_1 2\sqrt{\frac{\widetilde{m}_\mu}{\widetilde{m}_e}(1-\delta_\ell)}\cos\phi_a\right)},$$

$$\varepsilon_{13} = \frac{f_{\ell1}\left(1-\delta_\ell+\frac{\widetilde{m}_\mu}{\widetilde{m}_e}+\mathtt{s}_1 2\sqrt{\frac{\widetilde{m}_\mu}{\widetilde{m}_e}(1-\delta_\ell)}\cos\phi_a\right)}{(1-\delta_\ell)\left(1+\mathtt{s}_3\frac{\widetilde{m}_e}{\widetilde{m}_\mu}\right)(1+\mathtt{s}_2\widetilde{m}_e)},$$

$$\varepsilon_{12} = \frac{f_{\ell2}(1+\mathtt{s}_3(\delta_\ell-1))+f_{\ell1}\frac{\widetilde{m}_\mu}{\widetilde{m}_e}+f_{\ell1}(1-\delta_\ell)-2\mathtt{s}_1 f_{\ell1}\sqrt{\frac{\widetilde{m}_\mu}{\widetilde{m}_e}(1-\delta_\ell)}c_a+(-1)^i 2\left(\sqrt{(1+\mathtt{s}_3(\delta_\ell-1))(1-\delta_\ell)f_{\ell1}f_{\ell2}}c_c-\mathtt{s}_1\sqrt{\frac{\widetilde{m}_\mu}{\widetilde{m}_e}(1+\mathtt{s}_3(\delta_\ell-1))f_{\ell1}f_{\ell2}}c_{ac}\right)}{(1-\delta_\ell)\left(1+\mathtt{s}_3\frac{\widetilde{m}_e}{\widetilde{m}_\mu}\right)(1+\mathtt{s}_2\widetilde{m}_e)-\frac{\widetilde{m}_e}{\widetilde{m}_\mu}\frac{f_{\ell1}}{2}\left(1-\delta_\ell+\frac{\widetilde{m}_\mu}{\widetilde{m}_e}+\mathtt{s}_1 2\sqrt{\frac{\widetilde{m}_\mu}{\widetilde{m}_e}(1-\delta_\ell)}\cos\phi_a\right)},$$

(A.3)

where $i=0$ for $\mathbf{M}^2_\ell$, $i=1$ for $\mathbf{M}^4_\ell$.

Acknowledgments

"The authors thankfully acknowlegde computer resources, technical advice and support provided by Laboratorio Nacional de Supercómputo del Sureste de Mx́ico (LNS), a member of the CONAHCYT national laboratories, with proyect No. 202301024C."

This work has been partially supported by CONAHCYT-SNI (México).

1. M. C. Gonzalez-Garcia, Neutrinos Theory Review, *PoS* **ICHEP2012** (2013) 005, https://doi.org/10.22323/1.174.0005.

2. A. Gando *et al.* [KamLAND-Zen], Search for Majorana Neutrinos near the Inverted Mass Hierarchy Region with KamLAND-Zen, *Phys. Rev. Lett.* **117** (2016) 082503, https://doi.org/10.1103/PhysRevLett.117.082503. [arXiv:1605.02889 [hep-ex]].

3. Y. Abe *et al.*, [Double Chooz], Indication of Reactor $\bar{\nu}_e$ Disappearance in the Double Chooz Experiment, *Phys. Rev.*

Lett. **108** (2012) 131801, https://doi.org/10.1103/PhysRevLett.108.131801. [arXiv:1112.6353 [hep-ex]].

4. F. P. An *et al.*, [Daya Bay], Observation of electron-antineutrino disappearance at Daya Bay, *Phys. Rev. Lett.* **108** (2012) 171803, https://doi.org/10.1103/PhysRevLett.108.171803. [arXiv:1203.1669 [hep-ex]].
5. J. K. Ahn *et al.* [RENO], Observation of Reactor Electron Antineutrino Disappearance in the RENO Experiment, *Phys. Rev. Lett.* **108** (2012) 191802, https://doi.org/10.1103/PhysRevLett.108.191802. [arXiv:1204.0626 [hep-ex]].
6. P. F. de Salas *et al*., 2020 global reassessment of the neutrino oscillation picture, *JHEP* **02** (2021) 071, https://doi.org/10.1007/JHEP02(2021)071. [arXiv:2006.11237 [hep-ph]].
7. H. Fritzsch, Weak Interaction Mixing in the Six - Quark Theory, *Phys. Lett. B* **73** (1978) 317, https://doi.org/10.1016/0370-2693(78)90524-5.
8. H. Fritzsch, Quark Masses and Flavor Mixing, *Nucl. Phys. B* **155** (1979) 189, https://doi.org/10.1016/0550-3213(79)90362-6.
9. P. H. Frampton, S. L. Glashow and D. Marfatia, Zeroes of the neutrino mass matrix, *Phys. Lett. B* **536** (2002) 79, https://doi.org/10.1016/S0370-2693(02)01817-8. [arXiv:hep-ph/0201008 [hep-ph]].
10. P. O. Ludl and W. Grimus, A complete survey of texture zeros in the lepton mass matrices, *JHEP* **07** (2014) 090, [erratum: JHEP **10** (2014) 126] https://doi.org/10.1007/JHEP07(2014)090. [arXiv:1406.3546 [hep-ph]].
11. H. Fritzsch and Z. z. Xing, Mass and flavor mixing schemes of quarks and leptons, *Prog. Part. Nucl. Phys.* **45** (2000) 1-81, https://doi.org/10.1016/S0146-6410(00)00102-2. [arXiv:hep-ph/9912358 [hep-ph]].
12. S. Sharma, P. Fakay, G. Ahuja and M. Gupta, Finding a unique texture for quark mass matrices, *Phys. Rev. D* **91** (2015) 053004, https://doi.org/10.1103/PhysRevD.91.053004. [arXiv:1503.03963 [hep-ph]].
13. E. Barradas-Guevara, O. Félix-Beltrán and F. Gonzalez-Canales, Deviation to the Tri-Bi-Maximal flavor pattern and equivalent classes, *Int. J. Mod. Phys. A* **38** (2023) 2350031, https://doi.org/10.1142/S0217751X23500318. [arXiv:2204.03664 [hep-ph]], and therein references.
14. P. A. Zyla *et al.*, [Particle Data Group], Review of Particle Physics, *PTEP* **2020** (2020) 083C01, https://doi.org/10.1093/ptep/ptaa104.
15. M. Sajjad Athar *et al.*, Status and perspectives of neutrino physics, *Prog. Part. Nucl. Phys.* **124** (2022) 103947, https://doi.org/10.1016/j.ppnp.2022.103947. [arXiv:2111.07586 [hep-ph]].
16. P. F. Harrison, D. H. Perkins and W. G. Scott, Tri-bimaximal mixing and the neutrino oscillation data, *Phys. Lett. B* **530** (2002) 167 https://doi.org/10.1016/S0370-2693(02)01336-9. [arXiv:hep-ph/0202074 [hep-ph]].
17. V. D. Rusov, V. A. Tarasov, S. A. Chernegenko and V. P. Smolyar, Comment on 'Observation of electron-antineutrino disappearance at Daya Bay', [arXiv:1204.5974 [hep-ph]].
18. Y. H. Ahn, H. Y. Cheng and S. Oh, Recent Neutrino Data and a Realistic Tribimaximal-like Neutrino Mixing Matrix, *Phys. Lett. B* **715** (2012) 203-207 https://doi.org/10.1016/j.physletb.2012.07.061. [arXiv:1105.4460 [hep-ph]].
19. P. Chen, S. Centelles Chuliá, G. J. Ding, R. Srivastava and J. W. F. Valle, CP symmetries as guiding posts: revamping tri-bi-maximal mixing. Part I, *JHEP* **03** (2019) 036 https://doi.org/10.1007/JHEP03(2019)036. [arXiv:1812.04663 [hep-ph]].
20. E. Barradas-Guevara, O. Felix-Beltran, F. Gonzalez-Canales and M. Zeleny-Mora, Lepton CP violation in a ν2HDM with flavor, *Phys. Rev. D* **97** (2018) 035003 https://doi.org/10.1103/PhysRevD.97.035003. [arXiv:1704.03474 [hep-ph]].